Acta Neuropathologica (2020) 139:773–789
https://doi.org/10.1007/s00401-020-02125-x

ORIGINAL PAPER

Picalm reduction exacerbates tau pathology in a murine tauopathy model

Kunie Ando[1] · Robert De Decker[1] · Cristina Vergara[1] · Zehra Yilmaz[1] · Salwa Mansour[1] · Valérie Suain[1] · Kristel Sleegers[2] · Marie-Ange de Fisenne[1] · Sarah Houben[1] · Marie-Claude Potier[3] · Charles Duyckaerts[3,4] · Toshio Watanabe[5] · Luc Buée[6] · Karelle Leroy[1] · Jean-Pierre Brion[1]

Received: 13 September 2019 / Revised: 13 December 2019 / Accepted: 1 January 2020 / Published online: 10 January 2020

Abstract

Genome-wide association studies (GWAS) have identified *PICALM* as one of the most significant susceptibility loci for late-onset Alzheimer's disease (AD) after *APOE* and *BIN1*. PICALM is a clathrin-adaptor protein and plays critical roles in clathrin-mediated endocytosis and in autophagy. PICALM modulates brain amyloid ß (Aß) pathology and tau accumulation. We have previously reported that soluble PICALM protein level is reduced in correlation with abnormalities of autophagy markers in the affected brain areas of neurodegenerative diseases including AD, sporadic tauopathies and familial cases of frontotemporal lobar degeneration with tau-immunoreactive inclusions (FTLD-tau) with mutations in the microtubule-associated protein tau (*MAPT*) gene. It remains unclarified whether in vivo PICALM reduction could either trigger or influence tau pathology progression in the brain. In this study, we confirmed a significant reduction of soluble PICALM protein and autophagy deficits in the post-mortem human brains of FTLD-tau-*MAPT* (P301L, S364S and L266V). We generated a novel transgenic mouse line named Tg30xPicalm+/− by crossing Tg30 tau transgenic mice with Picalm-haploinsufficient mice to test whether Picalm reduction may modulate tau pathology. While Picalm haploinsufficiency did not lead to any motor phenotype or detectable tau pathology in mouse brains, Tg30xPicalm+/− mice developed markedly more severe motor deficits than Tg30 by the age of 9 months. Tg30xPicalm+/− had significantly higher pathological tau levels in the brain, an increased density of neurofibrillary tangles compared to Tg30 mice and increased abnormalities of autophagy markers. Our results demonstrate that Picalm haploinsufficiency in transgenic Tg30 mice significantly aggravated tau pathologies and tau-mediated neurodegeneration, supporting a role for changes in Picalm expression as a risk/sensitizing factor for development of tau pathology and as a mechanism underlying the AD risk associated to PICALM.

Keywords PICALM · Neurofibrillary tangles · Autophagy · Tau pathology · FTLD-tau-*MAPT* · GWAS

Electronic supplementary material The online version of this article (https://doi.org/10.1007/s00401-020-02125-x) contains supplementary material, which is available to authorized users.

✉ Kunie Ando
Kunie.Ando@ulb.ac.be

✉ Jean-Pierre Brion
jpbrion@ulb.ac.be

[1] Laboratory of Histology, Neuroanatomy and Neuropathology, UNI (ULB Neuroscience Institute), Faculty of Medicine, Université Libre de Bruxelles, 808 route de Lennik, Bldg GE, 1070 Brussels, Belgium

[2] Neurodegenerative Brain Diseases Group, VIB Center for Molecular Neurology, University of Antwerp, Universiteitsplein 1, 2610 Antwerp, Belgium

[3] Sorbonne Universités, UPMC Univ Paris 06 UMR S 1127, and Inserm, U 1127, and CNRS UMR 7225, and ICM, 75013 Paris, France

[4] Laboratoire de Neuropathologie Escourolle, Hôpital de La Pitié-Salpêtrière, AP-HP, Paris, France

[5] Department of Biological Science, Graduate School of Humanities and Sciences, Nara Women's University, Nara, Japan

[6] University of Lille, Inserm, CHU-Lille, Alzheimer and Tauopathies, LabEx DISTALZ, 59000 Lille, France

Introduction

Alzheimer's disease (AD) is the most common form of dementia. AD has two neuropathological lesions: senile plaques constituted of amyloid β (Aβ) peptide and neurofibrillary tangles (NFT) composed of intracellular tau aggregates. Genome-wide association studies (GWAS) have identified dozens of single nucleotide polymorphisms (SNPs) that are associated with higher or lower risk for late-onset Alzheimer's disease (LOAD). Yet, the mechanisms by which the proteins derived from GWAS-hit genes affect the disease risk remain largely unclear. The future challenges in the post-genomic era would be the determination of the mechanisms by which these genetic factors modulate disease aetiology. In this study, we focused on *PICALM* gene coding phosphatidylinositol-binding clathrin-assembly protein PICALM (also known as CALM). *PICALM* is one of the most significant susceptibility factors for LOAD after *APOE* and *BIN1* [24, 32, 33]. PICALM plays critical roles in clathrin-mediated endocytosis as a clathrin-adaptor protein [57]. Previously, we have reported that PICALM is associated with pathological tau in the brain of AD [3], PSP and Pick disease (PiD) [6]. PICALM protein level is decreased in the affected brain areas of various tau-related neurodegenerative diseases including AD, FTLD-tau with *MAPT* mutation at P301L, corticobasal degeneration (CBD) and Lewy body dementia (LBD) diffuse type with tau pathology. In these tauopathies, there is a significant negative correlation between PICALM protein level and hyperphosphorylated tau or autophagy initiation marker Beclin1 in the brain [6]. PICALM is a substrate of both calpain and caspase-3 [3, 28, 46] that are activated in the brain in AD and tauopathies [1, 16, 21, 47, 54, 60]. Together with sequestration by pathological tau, it is presumed that availability of functional PICALM proteins should be significantly reduced in these diseases. Previous studies suggest that PICALM is involved in the development of both amyloid and tau pathologies. PICALM regulates APP processing [27, 58, 59] and Aβ transcytosis [65]. PICALM has been reported to modulate tau degradation via both autophagosome formation and autolysosomal fusion in cultured cells, drosophila and zebrafish [38]. Nonetheless, it has never been analysed in a murine tauopathy model whether PICALM reduction can trigger or accelerate tau pathology and tau-mediated neurodegeneration. We hypothesized that PICALM reduction may cause or aggravate tau pathology progression. We first analysed post-mortem human brains and confirmed that soluble PICALM protein was reduced and autophagy activity was decreased in FTLD-tau-*MAPT* brains. We then set out to create a novel transgenic mouse line Tg30xPicalm+/− by crossing Tg30 tau transgenic mice [35] with Picalm+/− mice [55]. Tg30 mice develop cell autonomous tau pathology and severe motor deficits in an age-dependent manner [35]. Homozygous Picalm knockout mice are dwarfed and die within 1 month after birth due to deficiency in erythroid maturation and transferrin uptake [55] and thus were not used in this study. We observed that hemizygous Picalm loss without human mutant tau overexpression did not cause a clear motor phenotype or any detectable tau pathology. However, hemizygous Picalm loss in Tg30 tau transgenic mice led to aggravation of motor deficits. Biochemical and histochemical analyses suggest that tau pathology was exacerbated in the brain of Tg30xPicam+/− mice. Our data suggest that Picalm reduction acts as a sensitizing factor to accelerate tau pathology progression.

Materials and methods

Human brain tissues

For biochemical analysis, a total of ten samples were obtained post-mortem from control non-demented individuals ($n=5$) and FTLD-tau-*MAPT* ($n=5$) as listed in Table 1. Control cases were non-demented individuals who died without known neurological disorders. The mean age at death and post-mortem delays of control cases and of FTLD-tau-*MAPT* patients (Table 1) were not significantly different. Average age at death was 60.20 ± 2.34 years and 50.8 ± 4.4 years (mean ± s.e.m) for control and FTLD-tau-*MAPT* cases, respectively ($p=0.10$). Average post-mortem delays were 28.5 ± 0.5 h and 35.0 ± 7.5 h for control and FTLD-tau-*MAPT* cases ($p=0.60$). For immunohistochemistry, formalin-fixed and paraffin-embedded samples from two of the FTLD-tau-*MAPT* cases were available and were

Table 1 The clinical and genetic features of control subjects and of FTLD-tau patients (with identified *MAPT* tau mutations) used in this study are described

Case#	Clinical diagnosis	PMD (hours)	Age (years)	Sex
1	Control	ND	58	M
2	Control	28	60	F
3	Control	29	52	F
4	Control	ND	66	M
5	Control	ND	65	F
6	*FTLD-P301L*	49	50	F
7	*FTLD-P301L*	31	65	F
8	*FTLD-P301L*	44h30	48	F
9	*FTLD-P364S*	ND	53	M
10	*FTLD-L266V*	15h30	38	F

Frozen tissues of T1 isocortex were analysed by western blotting. Paraffin-embedded cortical brain sections of two FTLD-tau-*MAPT* cases (#7 and #10) were analysed by immunohistochemistry

FTLD frontotemporal lobar degeneration

analysed in this study. Some of the cases analysed in this study were enrolled in a brain donation program of the French national Brain Bank, GIE NeuroCEB (Bioresource Research Impact Factor number = BRIF BB-0033–00,011) organized by a consortium of Patients Associations. An explicit consent had been signed by the patient or by the next of kin, in the name of the patient. The project has been approved by the scientific committee of the Brain Bank. The consent form had been reviewed and accepted by the Ethical Committee "Comité de Protection des Personnes Paris Ile de France VI". The whole procedure has been certified by AFNOR (Association Française de Normalisation). The collection of post-mortem samples has been declared to the Ministry of Research and Higher Education as requested by the French law and the Brain Bank has been officially authorized to provide sample to scientists. The rest of the cases were collected and stored in the brain bank of the LHNN (BB190052) and the study using these post-mortem tissues was performed in compliance and following approval of the Ethical Committee of the Medical School of the Free University of Brussels.

Preparation of brain homogenates for biochemical analysis

Frontal or T1 isocortex from human post-mortem brains or mouse hemispheres were snap frozen and kept at − 80 °C. About 200 mg of brain tissue was homogenised in five volumes of ice-cold-modified RIPA buffer constituted of 50 mM Tris pH 7.4 containing 150 mM NaCl, 1% NP-40, 0.25% sodium deoxycholate, 5 mM EDTA, 1 mM EGTA, Roche complete protease inhibitors, 1 mM PMSF, and phosphatase inhibitor cocktail 2, (P-5726, Sigma) and incubated for 60 min at 4 °C on a rotator and was centrifuged (20,000 × *g* for 20 min at 4 °C) and the supernatant was used as an RIPA-soluble fraction [3]. The RIPA-insoluble pellet was re-suspended in fivefold volume of 8 M urea supplemented with 5 mM EDTA, 1 mM EGTA, Roche complete protease inhibitors, 1 mM PMSF, and phosphatase inhibitor cocktail 2 by vortex and sonication on ice and incubated for 30 min at room temperature on a rotator. The mixture was centrifuged at 20,000 × *g* at 4 °C for 20 min. The supernatant was used as RIPA-insoluble fraction.

Western blot (WB)

Protein concentrations were estimated by the Bradford method (Bio-Rad). Samples (20 µg/lane) were run in 10% or 15% Tris–glycine gels depending on the molecular weight of the protein of interest and transferred onto nitrocellulose (ultracruz, SCBT) or PVDF membranes (Bio-Rad). The membranes were blocked in 10% (w/v) semi-fat dry milk in TBS (Tris-buffered saline, 20 mM Tris pH 7.6, 150 mM NaCl) for 1 h at room temperature and were incubated with primary antibodies overnight at 4 °C. After three rinses with TBS-T (TBS supplemented with 0.05% Tween-20), the membranes were incubated with anti-rabbit (#7074, CST, Bioké) or anti-mouse (A6782, Sigma) immunoglobulin conjugated with horseradish peroxidase. After three rinses with TBS-T, the membranes were incubated with SuperSignal West Pico PLUS Substrate (Thermofisher) and were exposed to a DARQ-7 CCD cooled camera in a SOLO 4S WL system (Vilber-Lourmat). Levels of proteins were estimated by densitometry analysis using the NIH ImageJ program, and adjusted for protein loading based on WB performed with an anti-actin antibody.

Co-immunoprecipitation (IP) assay

Co-IP was performed using the RIPA-soluble fraction as previously described [3]. The RIPA-soluble fraction of T1 isocortex was pre-cleared for 1 h at 4 °C with pre-equilibrated Protein A Sepharose (P3391, Sigma) and centrifuged at 3000 × *g* to obtain input fraction. Input fraction was incubated with pre-equilibrated Protein A Sepharose and with 1 µg of the anti-PICALM HPA019053 antibody at 4 °C on a rotator overnight. The protein A Sepharose beads were pelleted and washed three times with RIPA buffer. After the third wash, SDS sample buffer containing 5% ß-mercaptoethanol was added to the beads. Samples were heated at 100 °C and PICALM immunoprecipitates were analysed by WB for the presence of hyperphosphorylated tau.

Generation of Tg30xPicalm+/− mice

Tg30xPicalm+/− mice were generated by crossing Tg30 mice and Picalm+/− mice. Tg30 mice express a 1N4R human tau isoform mutated at positions G272V and P301S, under control of a thy-1 promoter [35, 49]. The Picalm+/− line was generated by inserting PGK-neo-pA into the first exon of Picalm gene [55]. Both heterozygous Tg30 and hemizygous Picalm+/− mice were maintained into a C57BL6 background by back crossing at least five generations. The F1 Tg30 mice were then bred with Picalm+/− mice to generate F2 Tg30×Picalm+/− animals expressing human double mutant tau and bearing only one valid Picalm gene allele. Genotyping was performed by two independent PCR amplifications of DNA extracted from ear biopsies. Mice were genotyped for human mutant tau with the primers (forward 5′-ATG GCT GAG CCC CGC CAG GAG-3′, reverse 5′-TGG AGG TTC ACC AGA GCT GGG-3′) [49]. Mice were also genotyped for Picalm with Primer A (forward 5′-ATG TCT GGC CAG AGC CTG ACG GAC CGA ATC-3′) and C (reverse 5′-GGG TCG GGA GAG GAT GCG GGG GGT CTT CAC-3′) for wild-type allele and Neogt-1 (reverse 5′-CTG ACC GCT TCC TCG TGC TTT ACG-3′) for the knockout allele [55]. A total of 49

non-transgenic wild-type (WT), 56 Picalm+/−, 42 Tg30 and 39 Tg30×Picalm+/− were used in this study.

Rotarod test

Motor deficits were evaluated by testing them on a rotarod apparatus (Ugo Basile), as previously described [35]. Briefly, animals were first submitted to training sessions (three trials per day during 3 consecutive days) during which they were placed on the rod rotating with a progressive acceleration from 4 to 40 rpm. Animals were individually separated the day before the test and evaluated using the same experimental setting throughout 300 s. The latency to fall off the rotarod was recorded. Animals staying more than 300 s were removed from the rotarod and their latency was recorded as 300 s.

Wire hang test

The wire hang test was performed by placing mice on the top of a cage lid as previously described [18]. This lid was then turned upside down at a height of 20 cm above the cage litter for a maximum of 60 s. This test was carried out three times per day for 3 days. The latency to fall off the wire was recorded for each of the nine sessions and the mean latency was calculated.

Analysis of sarkosyl-insoluble PHF-tau fraction

1 ml of RIPA-soluble fraction was subjected to sarkosyl fractionation by incubating with 1% (wt/v) N-lauroylsarcosine (L-5125, Sigma) under mild rotation for 30 min at RT and centrifuged for 30 min at 100,000 × *g* at 4 °C as previously described [3]. The pellet after ultracentrifugation containing the sarkosyl-insoluble material was gently rinsed in 500 µl of PBS and suspended in 100 µl PBS. Sarkosyl-insoluble fraction was analysed by WB.

Histological staining and immunocytochemistry

Mouse brains were fixed in 10% formalin for 24 h before embedding in paraffin. Tissue Sects. (7 µm thick) were stained with the Gallyas silver-staining method to identify NFT [31]. They were examined with a Zeiss Axioplan microscope and digital images acquired using an Axiocam HRc camera. The immunohistochemical labelling was performed using the ABC method (Elite) as previously reported [4]. Briefly, deparaffinised tissue sections were treated with H_2O_2 to inhibit endogenous peroxidase and incubated with the blocking solution of 10% (v/v) normal horse serum in TBS (0.01 M Tris, 0.15 M NaCl, pH 7.4). After an overnight incubation with the diluted primary antibody, the sections were sequentially incubated with either horse anti-mouse or goat anti-rabbit antibodies conjugated to biotin (Vector) followed by the ABC complex (Vector). The peroxidase activity was developed using diaminobenzidine (Dako) as chromogen. Double immunolabelling was performed using fluorescent markers. The first antibody was detected using an anti-mouse antibody conjugated to Alexa 594 (Molecular Probes). The second antibody was detected using an anti-rabbit antibody conjugated to HRP (CST, Bioké), followed by detection with Tyramide-FITC kit (Perkin Elmer). Double immunolabelling was followed by nuclear DAPI staining. The slides were mounted with Fluoromount-G (Southern biotech) and were observed with an Axiovert 200 M microscope (Zeiss) equipped with an ApoTome system (Zeiss). For quantitative analysis, Gallyas-positive or AT8-positive neurons in hippocampal Ammon's horn and dentate gyrus were counted on sagittal sections at a lateral level approximately 1 mm from the midline (Allen brain atlas) with a 40X objective as reported previously in Tg30 mice [35]. To analyse the pons and the motor areas (M1 and M2) of the cortex, the density of cells labelled for Gallyas, AT8, phosphorylated neurofilament heavy chain (pNF-H) and p62 was assessed on 10X images by thresholding analyses using NIH ImageJ as previously reported [61]. Area fractions were calculated by measuring the labelled area divided by the total surface of the area analysed.

Antibodies

The rabbit polyclonal anti-PICALM HPA019053 antibody was purchased from Sigma. The rabbit polyclonal anti-total tau antibody (A0024) was purchased from Dako (Agilent, Belgium). The rabbit polyclonal anti-total tau B19 antibody was raised to adult bovine tau proteins and reacts with all known adult and foetal tau isoforms in bovine, rat, mouse and human nervous tissue in a phosphorylation-independent manner [8]. The rabbit polyclonal BR21 antibody against human tau was generated by immunizing rabbits with the synthetic peptide C-GTYGLGDRKDQGG conjugated to PPD, corresponding to residues 16–28 in the amino-terminal region of tau (in exon 1), with the addition of an amino-terminal cysteine [5]. The mouse monoclonal PHF1 antibody (kindly provided by Dr P. Davies) is specific for tau phosphorylated at Ser396/404 [42]. The AT8 mouse monoclonal antibody was purchased from ThermoFisher (Belgium) and is specific for tau phosphorylated at Ser202 and Thr205 (AT8) [19]. The mouse monoclonal AP422 antibody (kindly provided by Drs M. Hasegawa and M. Goedert, Cambridge, UK) recognises pSer422 of tau [25]. The following additional mouse monoclonal antibodies were also used: against ß-actin (clone AC15, Sigma), cdk5 (clone DC17, SCBT), and GSK3ß (TPK1, Transduction Laboratories). The following rabbit polyclonal antibodies were also used: against Beclin1 (H-300, SCBT), LC3B (NB600-1384, Novus),

pNF-H (NA1211, Affiniti, Exeter, UK), p35 (C-19, SCBT), GSK3α/β phosphorylated on Tyr279 or Tyr216 (BioSource) and p62 (NBP1-48,320, Novus).

Statistical analysis

Numbers of samples are indicated in the figure legend. Statistical analysis was performed using the Prism program (Graphpad Software). Statistical comparisons were performed using unpaired two-tailed Student *t* tests, one-way ANOVA with Turkey post-test comparisons or two-way ANOVA with Bonferroni post-tests as noted in figure legends. Values of $p < 0.05$ were considered significant.

Results

Soluble PICALM protein is reduced and autophagy activity is decreased in FTLD-tau-*MAPT* brains

We first analysed the protein level of PICALM in human post-mortem brains of FTLD-tau cases with *MAPT* mutations at P301L, P364S and L266V (Table 1). The results suggest that there was a consistent reduction of soluble PICALM protein level of PICALM species at 65 to 75 kDa down to 42.5 ± 8% compared to non-demented control samples 100 ± 19% (Fig. 1a, b) in the RIPA-soluble fraction of the T1 isocortex lysates of FTLD-tau-*MAPT*. Two

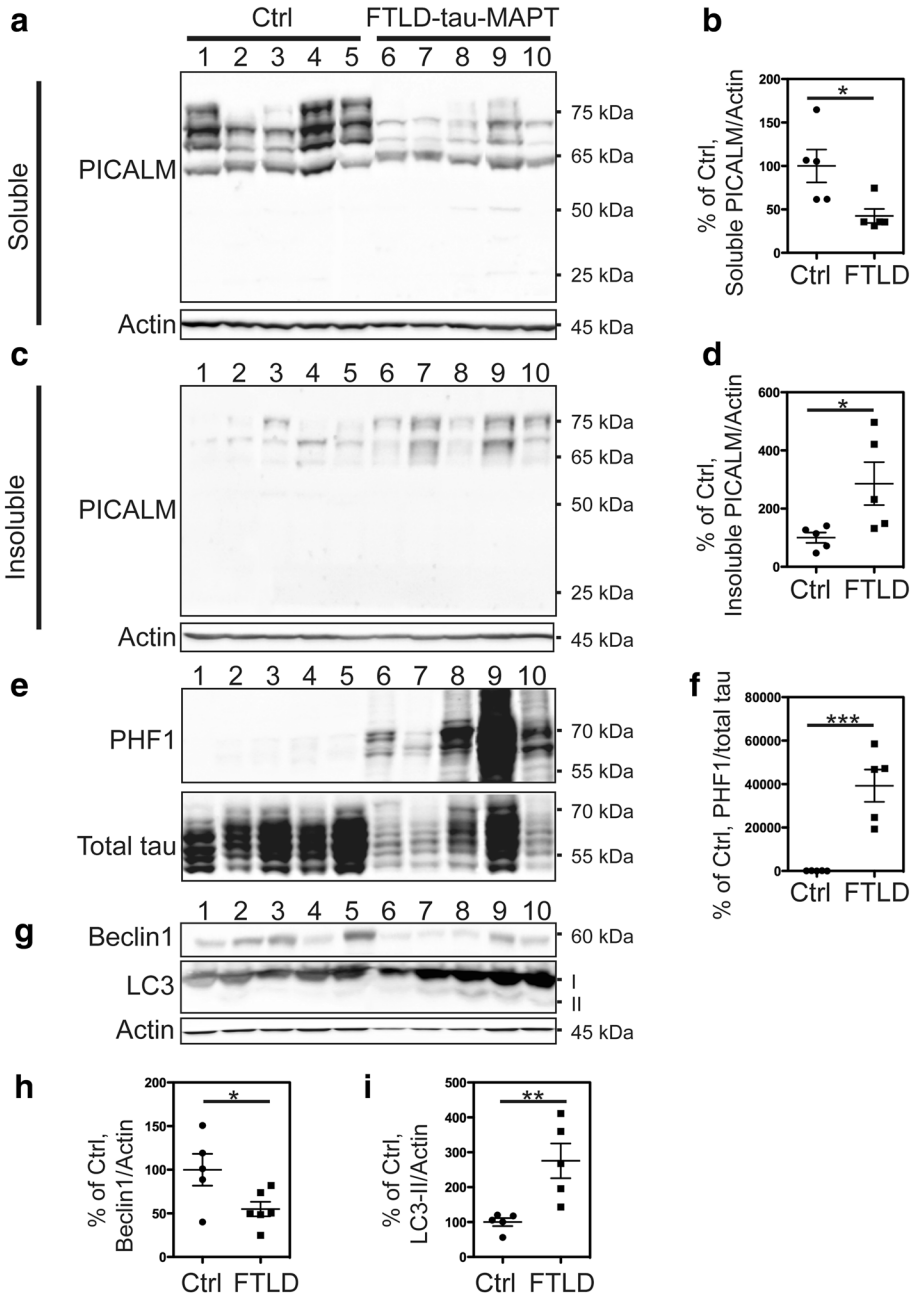

Fig. 1 Soluble PICALM protein level is decreased in the brain lysate of FTLD-tau with *MAPT* mutations. **a** RIPA-soluble fraction of temporal cortex extracts from five controls (Ctrl) and five FTLD-tau-*MAPT* cases was analysed by WB using antibodies against PICALM and loading control actin. Two FTLD-tau-*MAPT* cases (#8, and #9) had weak bands corresponding to cleaved PICALM fragments around 50 and/or 25 kDa in the RIPA-soluble fraction. **b** Quantification of expression level of PICALM protein normalised to actin of RIPA-soluble fraction. **c** RIPA-insoluble fraction was analysed by WB analysis using antibodies against PICALM and loading control actin. **d** Quantification of expression level of PICALM protein normalised to actin of RIPA-insoluble fraction. **e** RIPA-soluble fraction was analysed by WB using antibodies against PHF1 (pSer396/Ser404 tau) and total tau (Dako). **f** Quantification of hyperphosphorylated tau protein detected by PHF1 normalised to total tau. 100% is given to the average of control non-demented samples. **g** RIPA-soluble fraction was analysed by WB using antibodies against Beclin1, LC3 and loading control actin. **h** Quantification of Beclin1 normalised to actin. **i** Quantification of LC3-II normalised to actin. (Ctrl: $n = 5$, FTLD-tau-*MAPT*: $n = 5$. *$p < 0.05$, **$p < 0.01$, ***$p < 0.001$ by unpaired *t* test)

FTLD-tau-*MAPT* cases (#8 and #9) with highest phosphorylated tau levels (Fig. 1e) had cleaved PICALM fragments weakly detected around 50 and/or 25 kDa in the RIPA-soluble fraction (Fig. 1a) as previously observed in AD brain lysates [3]. On the contrary, PICALM detected in the RIPA-insoluble fraction was significantly increased in FTLD-tau-*MAPT* (Fig. 1c, d) [6]. There was a significant increase of PHF1-positive hyperphosphorylated tau in the brain lysates of FTLD-tau-*MAPT* patients (Fig. 1e, f) where no amyloid pathology was observed (data not shown). The autophagy initiation marker Beclin1 was decreased (Fig. 1g, h), while the autophagy flux marker LC3-II was increased in FTLD-tau-*MAPT* brains (Fig. 1g, i) [6].

The neuropathological phenotypes of the FTLD-tau with *MAPT* mutations are highly heterogeneous [17]. *MAPT* P301L mutation leads to formation of predominantly Gallyas-negative pretangles and globular glial tauopathy composed of 4-repeat (4R) tau [2, 17]. *MAPT* P364S mutation leads to a formation of composite neuronal tau inclusions (CNTI) constituted of both 3R and 4R tau [45]. *MAPT* L266V mutation leads to PiD phenotype [29]. Different mutations in the *MAPT* gene led to distinct molecular interaction between PICALM and tau (Supplementary Fig. 1a–g, online resource). Co-IP assay using anti-PICALM antibody suggested that phosphorylated tau was co-precipitated with PICALM in the brain lysates of case #9 (P364S) and #10 (L266V), but not clearly in the cases of FTLD-tau-*MAPT*-P301L (Supplementary Fig. 1a, online resource). A double immunofluorescence staining for PICALM and PHF1-positive phosphorylated tau on available paraffin sections (case #7 and #10) suggested that PICALM immunoreactivity was detected in approximately

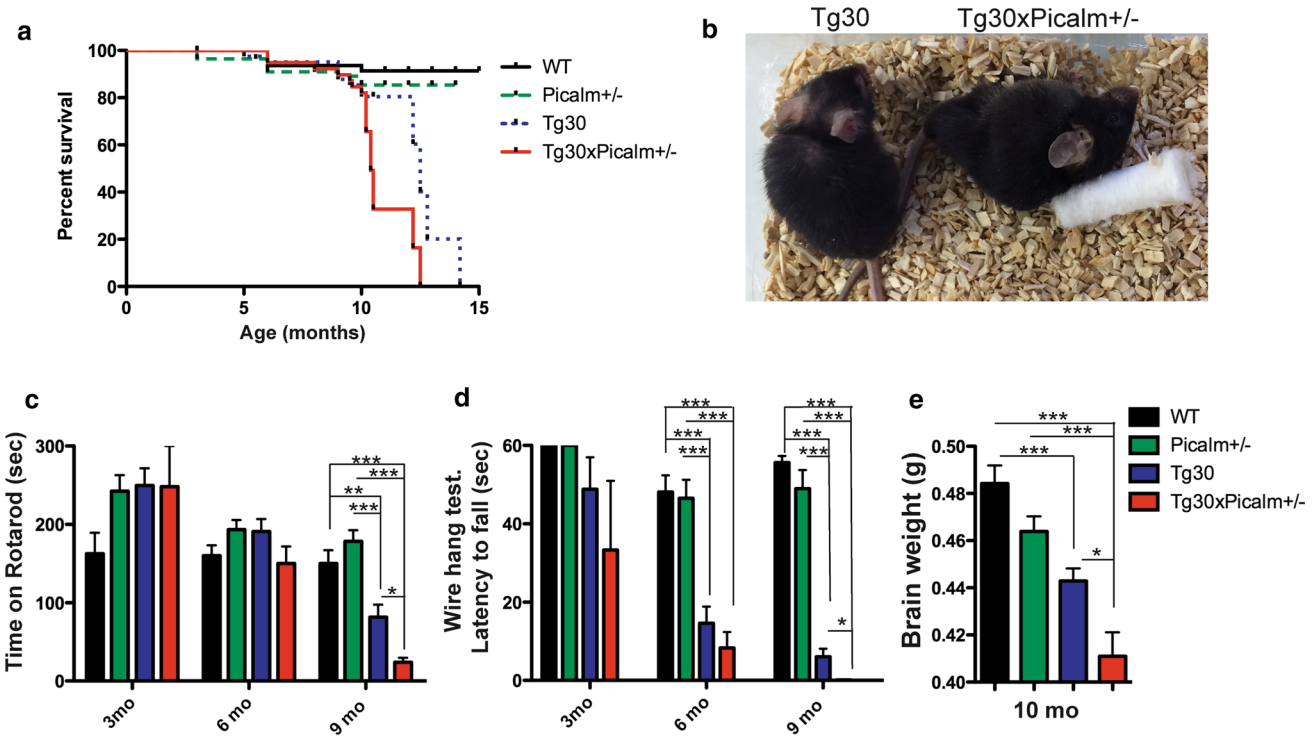

Fig. 2 Neurological defects are aggravated in Tg30xPicalm+/− compared to Tg30. **a** Kaplan-Maier survival curves of male and female WT, Picalm+/−, Tg30 and Tg30xPicalm+/− mice are shown ($n=49$, $n=56$, $n=42$, $n=39$, respectively). Tg30 and Tg30xPicalm+/− showed a significantly reduced survival compared with WT and Picalm+/− mice (by log-rank comparison, $***p<0.001$). **b** A representative photo of 11-month-old male Tg30 and Tg30xPicalm+/− mice is shown. Tg30xPicalm+/− mice exhibited an aggravated motor phenotype, abnormal gait and paralysis than Tg30 (see also Supplementary movie 1, online resource). **c** Performance on accelerated rotarod of male WT, Picalm+/−, Tg30 and Tg30xPicalm+/− is shown ($n=24$, $n=32$, $n=24$, $n=18$, respectively). At 9 months, both Tg30 and Tg30xPicalm+/− mice had significantly shorter time on rotating rotarod compared to WT and Picalm+/−. Tg30xPicalm+/− had significantly shorter time on rotarod than Tg30. **d** Wire hang test. Time of male WT, Picalm+/−, Tg30 and Tg30xPicalm+/− to fall from a suspended grid is shown ($n=24$, $n=32$, $n=24$, $n=18$, respectively). From 6 months, Tg30 and Tg30xPicalm+/− mice had significantly reduced latency on hanging wire compared to WT and Picalm+/− littermates. At 9 months, Tg30xPicalm+/− had significantly shorter latency on hanging wire than WT, Picalm+/− and Tg30 littermates. **e** Wet brain weight was measured just after the dissection of 10 month-old male WT, Picalm+/−, Tg30 and Tg30xPicalm+/− mice ($n=12$, $n=12$, $n=7$, $n=5$, respectively). Tg30xPicalm+/− had significantly reduced brain weight than Tg30. Data are represented as mean +/− SEM ($*p<0.05$, $**p<0.01$, and $***p<0.001$ by two-way ANOVA with Bonferroni post-tests for **c**, **d** and one-way ANOVA with Turkey post-tests for **e**). See also supplementary Fig. 2 and movie 1, online resource, for additional data

40% of Pick-like tau lesions of case #10 (L266V) but not in case #7 (P301L) (Supplementary Fig. 1b–g, online resource). Activated microglial cells were numerous and highly immunoreactive for PICALM in these FTLD-tau-*MAPT* cases (Supplementary Fig. 1d, g, online resource, white arrows). In spite of the heterogeneous interaction between PICALM and phosphorylated tau, there was a constant reduction of soluble PICALM protein level and abnormalities in autophagy markers in the FTLD-tau-*MAPT* brain. These data led us hypothesize that tauopathy in FTLD-tau-*MAPT* is associated to a significant reduction of clathrin-adaptor PICALM as well as to deregulation of autophagy and led us wonder if such aberrant reduction of PICALM could play a role in tau pathology progression.

Picalm reduction aggravates motor deficits in Tg30 tau transgenic mice

To determine whether the reduction of Picalm affects tau pathology and tau-related neuropathology, we used the well-characterized Tg30 tauopathy mouse model overexpressing 1N4R human tau-bearing double FTLD-related *MAPT* mutations at P301S and G272V [35]. To test the hypothesis that Picalm reduction modulates tau pathology progression, a novel transgenic mouse line named Tg30xPicalm+/− was created by crossing Tg30 mice [35] and Picalm+/− mice [55]. Tg30 mice developed NFTs from 3 months of age and exhibited severe motor deficits around 8 months, and generally die within 15 months [35]. Progeny were genotyped

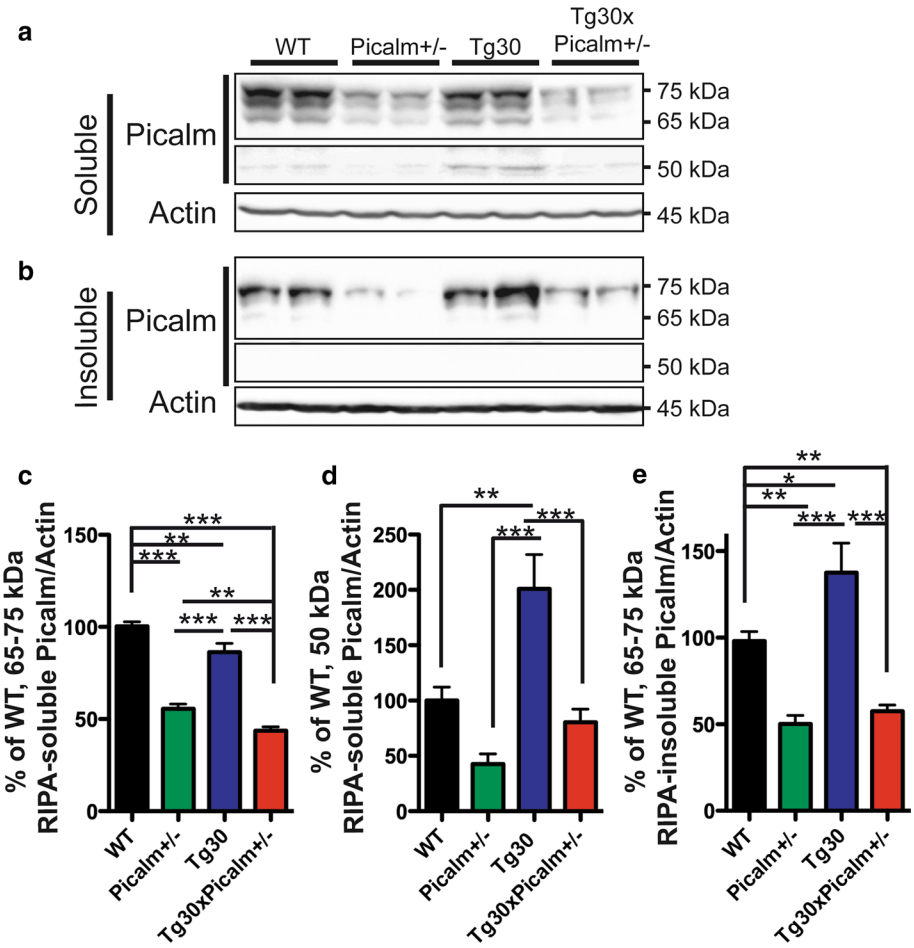

Fig. 3 Expression levels of Picalm in the brains of WT, Picalm+/−, Tg30 and Tg30xPicalm+/− at 10 months. Sex-matched 10-month-old mouse brains were analysed by WB (n = 12 per genotype). **a** WB analyses show the protein levels of Picalm species at 65–75 kDa or at 50 kDa (with a long exposure) and actin in the RIPA-soluble or RIPA-insoluble fraction. **b** Picalm species at 65–75 kDa or 50 kDa (not detected even after a long exposure) and actin in the RIPA-insoluble fraction. **c**, **d** Quantification of normalised level of 65–75 kDa Picalm (**c**) or 50 kDa- Picalm fragment (**d**) in RIPA-soluble fraction. There was approximately a 50% reduction of Picalm in Picalm+/− and Tg30xPicalm+/− mice. The 50 kDa- Picalm fragment in RIPA-soluble fraction was increased in Tg30 compared to WT mice. **e** Quantification of normalised 65–75 kDa Picalm in RIPA-insoluble fraction. The level of RIPA-insoluble Picalm was increased in Tg30 compared to WT. 100% is given to WT. Sex-matched samples were loaded onto the gels. **c**–**e** Data are represented as mean +/− SEM (*$p < 0.05$, **$p < 0.01$ and ***$p < 0.001$ by one-way ANOVA with Turkey post-tests)

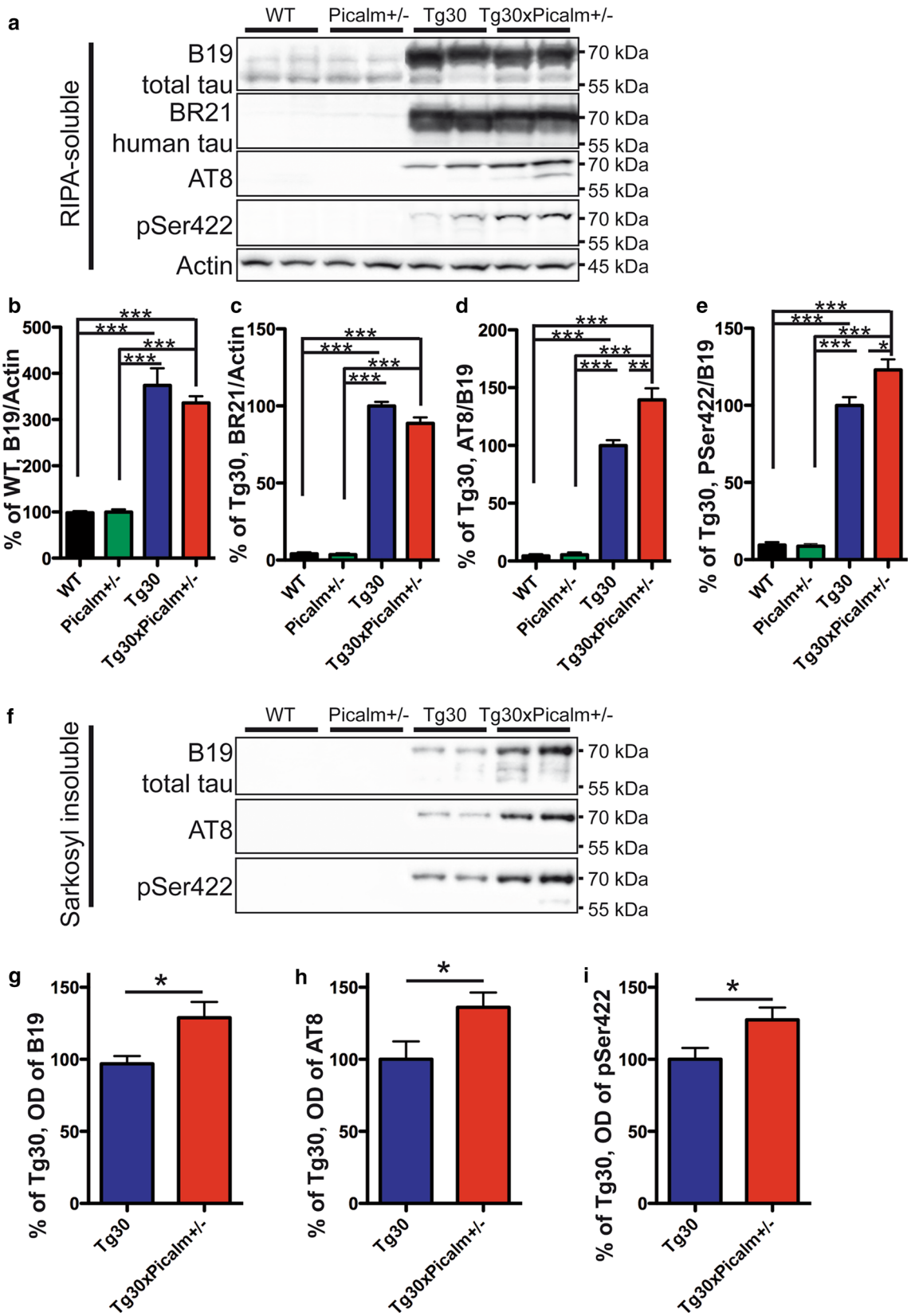
a
WT
Picalm+/-
Tg30
Tg30xPicalm+/-
RIPA-soluble
B19
total tau
BR21
human tau
AT8
pSer422
Actin
70 kDa
55 kDa
45 kDa
b
% of WT, B19/Actin
c
% of Tg30, BR21/Actin
d
% of Tg30, AT8/B19
e
% of Tg30, PSer422/B19
f
Sarkosyl insoluble
g
% of Tg30, OD of B19
h
% of Tg30, OD of AT8
i
% of Tg30, OD of pSer422

◂**Fig. 4** Picalm reduction is associated with increased phosphorylation and aggregation of tau in the brain of Tg30xPicalm+/− at 10 months. **a** Sex-matched 10-month-old mouse brains were analysed by WB ($n=12$ per genotype). WB analyses show the protein levels of total tau (B19), human tau (BR21), AT8 (pSer202/Thr205 tau), pSer422 tau and actin in the RIPA-soluble fraction. **b–e** Quantification of the levels of total tau normalised to actin (**b**), human tau normalised to actin (**c**), AT8 normalised to B19 (**d**) or pSer422 normalised to B19 (**e**). The levels of total tau and of human tau are not different between Tg30 and Tg30xPicalm+/− mice but phosphorylated tau is increased in Tg30xPicalm+/− compared to Tg30 mice. $*p<0.05$, $**p<0.01$ and $***p<0.001$ by one-way ANOVA with Turkey post-tests. **f** WB analyses of sarkosyl-insoluble, aggregated tau in the mouse brains at 10 months. (WT: $n=10$, Picalm+/−: $n=10$, Tg30: $n=12$ and Tg30x-Picalm+/−: $n=12$). **g–i** Quantification of the levels of sarkosyl-insoluble total tau (B19, **g**) or phosphotau (AT8, **h**) and (pSer422, **i**). 100% was given to the average of the optical density (OD) in Tg30 mice. Data are represented as mean +/− SEM. The level of sarkosyl-insoluble tau was increased in the brain of Tg30xPicalm+/− compared to Tg30. There was no detectable level of tau in the sarkosyl-insoluble fractions of WT or Picalm+/− mice. $*p<0.05$ by unpaired *t* test

to non-transgenic WT, Picalm+/−, Tg30 and Tg30xPicalm+/−. Tg30xPicalm+/− mice were born in slightly less than normal Mendelian ratio (WT: Picalm+/−: Tg30: Tg30xPicalm+/− =26.3:30.1:22.6:21.0).

Picalm+/− mice had normal body size and exhibited no obvious abnormalities without any motor deficits at least up to 9 months (Fig. 2). However, the mortality of female Picalm+/− mice was increased after pregnancy in our conventional animal house. Therefore, male Picalm+/− mice were systematically crossed with female Tg30 mice to avoid premature death of female Picalm+/− mice. The mice used for reproduction were excluded from the analyses of survival curve. Male Tg30 and Tg30×Picalm+/− mice died younger than female mice (Supplementary Fig. 2a, b, online resource). Tg30 and Tg30×Picalm+/− mice had significantly reduced life expectancy compared to WT or Picalm+/− littermates (Fig. 2a). Tg30×Picalm+/− mice had generally but not significantly shorter lifespan than Tg30 mice (Fig. 2a). From 6 months, both Tg30 and Tg30×Picalm+/− had a significant body weight loss compared to WT or Picalm+/− littermates but there was no significant difference between Tg30 and Tg30xPicalm+/− (Supplementary Fig. 2c, d, online resource).

Both Tg30 and Tg30xPicalm+/− developed severe motor deficits from 9 months old. Tg30×Picalm+/− had significantly worse performance by rotarod test or wire hang test than Tg30 littermates at 9 months (Fig. 2c, d). Memory tests could not be assessed at this age due to severe motor deficits of Tg30 and Tg30×Picalm+/− mice. At 11 months, Tg30×Picalm+/− were more paralyzed with abnormal unsteady gait (Fig. 2b) and suffered from severer paralysis and motor problems than Tg30 (Supplementary movie 1, online resource). Most of the mice were sacrificed at 10 months for biochemical and histological analyses. There was a significant reduction in brain weight in Tg30×Picalm+/− mice compared to WT, Picalm+/− and Tg30 (Fig. 2e). These results suggest that Picalm+/− mice did not exhibit any motor phenotype compared to WT but Tg30×Picalm+/− exhibited significantly aggravated motor phenotype compared to Tg30 littermates at rather late stage of their life.

Soluble PICALM protein level is decreased in the presence of human mutant tau overexpression

Alteration of Picalm protein expression was confirmed by WB. Mice were sacrificed at 10 months of age and the brains were homogenized in RIPA buffer. RIPA-soluble fraction was first analysed by WB for Picalm and actin as loading control (Fig. 3a). There was approximately 50% reduction of Picalm protein expression in Picalm+/− and Tg30×Picalm+/− mouse brains. Normalised Picalm protein in RIPA-soluble fraction was slightly reduced in the presence of human mutant tau overexpression (WT: Tg30 = 100 ± 2.5:86.3 ± 4.8 and Picalm+/−: Tg30×Picalm +/− =55.5 ± 2.9:43.7 ± 2.1) (Fig. 3c). On the contrary, the 50 kDa Picalm fragment, weakly detected after a prolonged exposure time, was increased in Tg30 mouse brains compared to WT (Fig. 3a, d). To verify potential changes of Picalm partitioning between soluble and insoluble fractions, RIPA-insoluble pellet was solubilized by sonication in 8 M urea buffer to dissociate large protein aggregates (Fig. 3b). The level of RIPA-insoluble Picalm was increased in Tg30 compared to WT (Fig. 3e), suggesting that tau pathology led to a reduction of soluble Picalm protein level and to an increase of insoluble Picalm in mouse brains as observed in the human brains of AD, primary tauopathies [6] and in FTLD-tau-*MAPT* cases (Fig. 1a–d). PICALM was accumulated in tau positive inclusions of human AD brains [3], PSP, PiD, LBD [6] and FTLD-tau-*MAPT*-L266V (Supplementary Fig. 1e–g, online resource). Indeed, Picalm protein was accumulated in some of the phosphotau-positive inclusions of mature NFTs in the cortex and brainstem of Tg30 mouse brains (Supplementary Fig. 3, online resource).

Haploinsufficiency of Picalm accelerated tau phosphorylation in Tg30xPicalm+/− brains

In the brains of Tg30 and Tg30×Picalm+/−, total tau protein level was estimated to be more than threefold compared to non-transgenic WT or Picalm+/− littermates due to overexpression of human tau protein. There was, however, no significant difference between Tg30 and Tg30×Picalm+/− in the levels of total tau or human tau detected in the RIPA-soluble fraction (Fig. 4a–c). To begin assessing the potential impact of Picalm haploinsufficiency

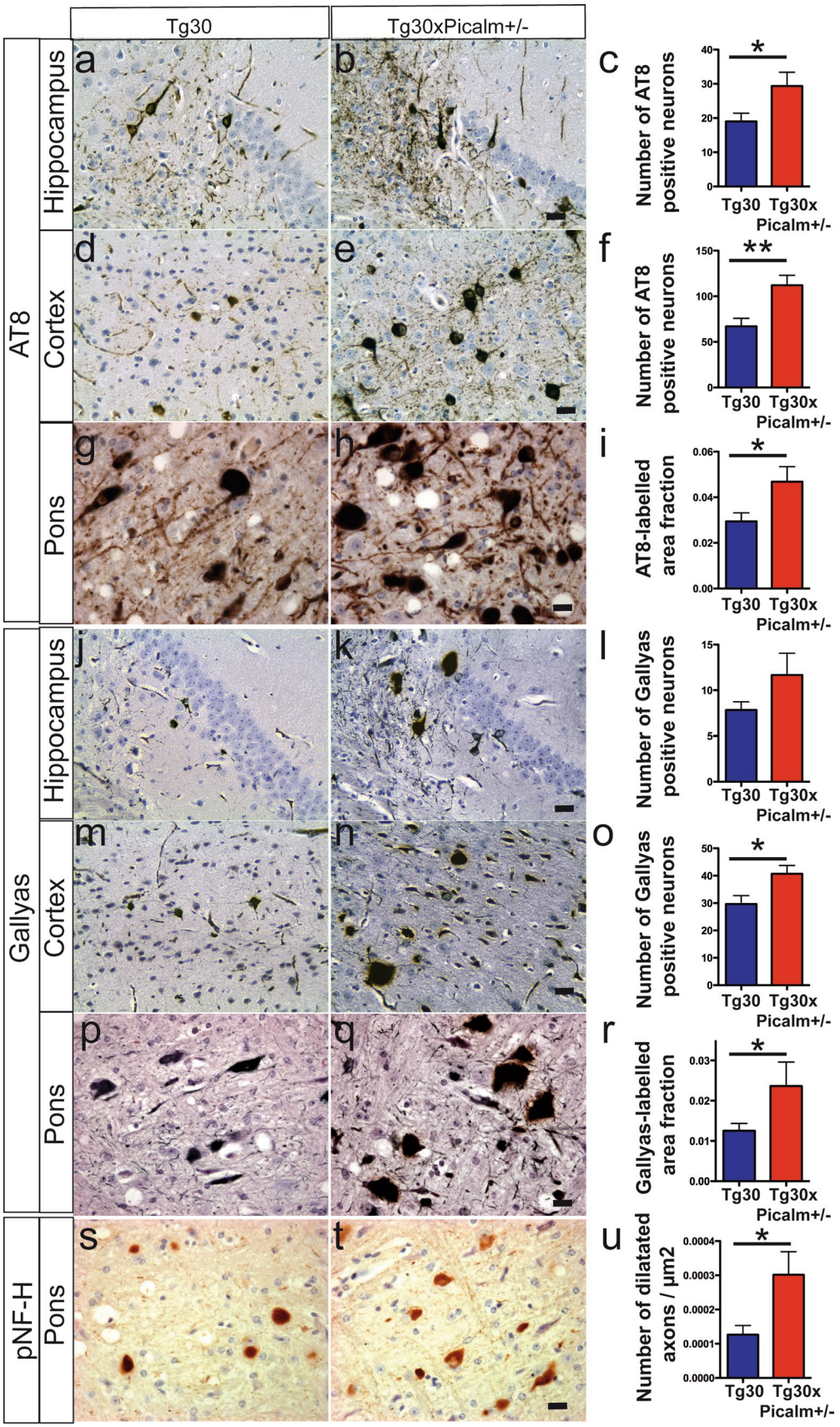
Tg30
Tg30xPicalm+/-
AT8
Hippocampus
Cortex
Pons
Gallyas
Hippocampus
Cortex
Pons
pNF-H
Pons
a
b
c
d
e
f
g
h
i
j
k
l
m
n
o
p
q
r
s
t
u
Number of AT8 positive neurons
Number of AT8 positive neurons
AT8-labelled area fraction
Number of Gallyas positive neurons
Number of Gallyas positive neurons
Gallyas-labelled area fraction
Number of dilatated axons / µm2
Tg30
Tg30x Picalm+/-
*
**

◂**Fig. 5** Picalm reduction enhances the development of neurofibrillary pathology. **a–i** Representative pictures of AT8 labelling of the hippocampus (**a, b**), cortex (**d, e**) and pons (**g, h**) of Tg30 and Tg30xPicalm+/−. There was a significant increase of the number of AT8-positive neurons (**c, f, i**) in Tg30xPicalm+/− compared to Tg30 in these three areas. **j–r** Representative photos of Gallyas silver staining of the hippocampus (**j, k**), cortex (**m, n**) and pons (**p, q**) of Tg30 and Tg30xPicalm+/−. There was a significant increase of the number of Gallyas-positive neurons in the cortex and pons (**o, r**) in Tg30xPicalm+/− compared to Tg30. **s-u** Representative pictures of immunolabelling of pNF-H in the pons (**s, t**). There was a significant increase of pNF-H-positive neurons in the pons of Tg30xPicalm+/− (**u**) compared to Tg30. Ten-month-old male mice (Tg30: $n=12$ and Tg30xPicalm+/−: $n=9$) were analysed. Data are represented as mean +/− SEM (*$p<0.05$, **$p<0.01$ by unpaired t tests). Scale bar 10 µm

on tau pathology, we examined by WB whether levels of hyperphosphorylated tau were affected. In WT and Picalm+/− mouse brain lysates, there was no detectable signal of AT8 or pSer422 positive tau. In RIPA-soluble fraction, tau proteins phosphorylated at pSer202/Thr205 (AT8) and pSer422 were present in both Tg30 and in Tg30xPicalm+/− mouse brain lysates but were significantly increased in Tg30xPicalm+/− compared to Tg30 (Fig. 4d, e).

Haploinsufficiency of Picalm promotes formation of tau aggregates in Tg30xPicalm+/− mouse brains

We next examined whether Picalm protein reduction could promote tau aggregate formation in the brain. Lysates of the brain hemispheres of 10-month-old WT, Picalm+/−, Tg30 and Tg30×Picalm+/− mice were processed by a sarkosyl fractionation method to obtain highly enriched fraction of aggregated tau [20]. Tau in the sarkosyl-insoluble fraction has been shown by immunoelectron microscopy to be filamentous [9]. In the sarkosyl-insoluble fractions, hyperphosphorylated tau protein was detected in Tg30 and Tg30xPicalm+/− mouse brains but not in the brain of WT and Picalm+/− (Fig. 4f). The levels of phosphorylated tau positive for AT8, pSer422 or B19 positive total tau were significantly increased in the sarkosyl-insoluble fraction of Tg30xPicalm+/− compared to Tg30 littermates (Fig. 4g–i).

Immunohistochemistry for AT8 indicated increased phosphotau-positive neuron density in Tg30xPicalm+/− mouse brains compared to Tg30 in the hippocampus, cortex and pons (Fig. 5a–i). Gallyas silver-staining method allowed detection of argyrophilic-aggregated proteins [31]. The number of Gallyas-positive NFTs was significantly increased in the brain cortex and pons of Tg30×Picalm+/− mouse brains compared to Tg30 (Fig. 5j–r). Axonopathy precedes tau pathology in the brainstem of Tg30 mouse model [35]. There were more numerous axonal dilatations and spheroids detected by anti-phospho neurofilament pNF-H antibody in the pons of Tg30×Picalm+/− compared to Tg30 (Fig. 5s–u). No detectable pathology was observed by immunohistochemical labelling for tau or pNF-H in WT or Picalm+/− mouse brains up to 10 months. Taken together, Picalm haploinsufficiency itself did not cause any obvious tau pathology, but Picalm haploinsufficiency in tau transgenic model led to significant increase of tau pathology in Tg30xPicalm+/− mouse brains compared to Tg30 littermates.

Reduced autophagy initiation and autophagosome fusion in Tg30xPicalm ± mouse brains

PICALM is a modulator of both autophagosome formation and autophagosome-lysosome fusion [38] via direct interaction with R-SNARE proteins [37]. To test the hypothesis that accelerated tau pathology in Tg30×Picalm+/− is related to autophagy dysfunctions in transgenic tau mouse brains, the levels of autophagy markers Beclin1 and LC3-II were measured in the brain lysates. The levels of Beclin1 and LC3-II were not significantly altered in Picalm+/− mouse brains compared to WT littermates (Fig. 6a–c). Nevertheless, in Tg30×Picalm+/− mouse brains, the autophagy initiation marker Beclin1 was decreased (Fig. 6b), suggesting that autophagy initiation was reduced compared to WT littermates. Also, there was a significant increase of the level of autophagy flux marker, LC3-II in Tg30×Picalm+/− mouse brains compared to WT and Picalm+/− littermates (Fig. 6c), suggesting that autophagosome degradation is reduced in Tg30xPicalm+/− mouse brains. The inhibition of autophagy in Tg30xPicalm+/− led to accumulation of autophagic substrates observed as p62 positive intraneuronal inclusions in the brain stem of Tg30×Picalm+/− mice (Fig. 6d–h). Taken together, hemizygous Picalm loss itself had no obvious effect on autophagy in mice, but Picalm haploinsufficiency in the presence of tau pathology led to a significant impairment of autophagy initiation and flux in mouse brains.

Accelerated conversion from p35 to p25 in Tg30xPicalm+/− mouse brains

Picalm is a substrate of both calpain and caspase-3 [3, 28, 46] and there was an increase of the level of cleaved Picalm protein at 50 kDa in Tg30 and Tg30xPicalm+/− mice (Fig. 3d). Calpain also converts p35 to p25 and this conversion increases cdk5 kinase activity [34]. In Tg30×Picalm+/− mouse brains, the level of cdk5 was not changed, but the level of p25 normalised to p35 was significantly increased (Fig. 7a–c). The level of active form of GSK3ß phosphorylated at Tyr216 was also significantly increased in Tg30xPicalm +/− mouse brains without a change in total protein level of GSK3ß (Fig. 7d, e). These data suggest that Tg30xPicalm+/− mice had an increased level of the active form of

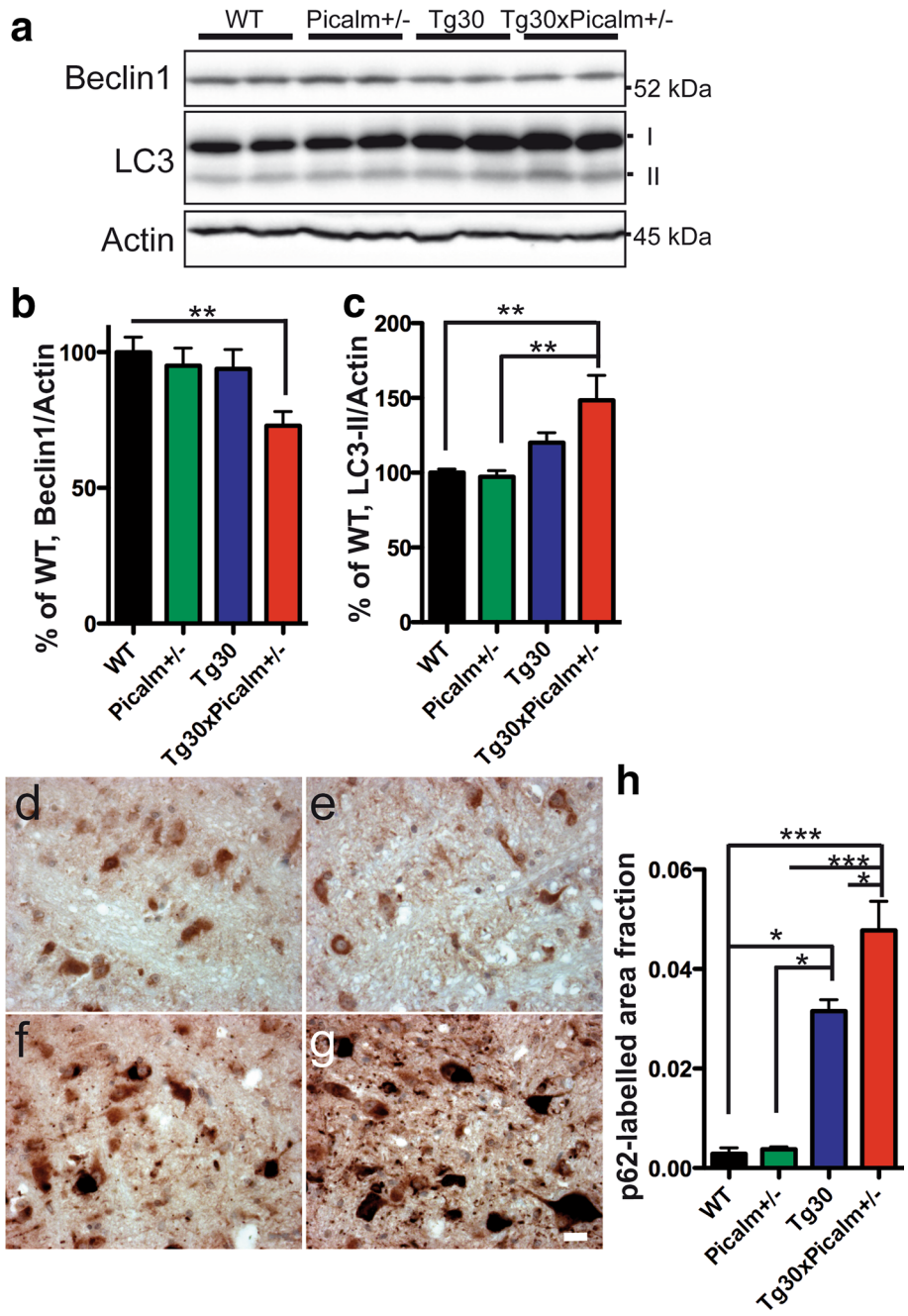

Fig. 6 Picalm reduction alters autophagy function in the presence of tau pathology. **a** Sex-matched 10-month-old mouse brains were analysed by WB ($n=12$ per genotype). WB analyses showing the expression of Beclin1, LC3-II and actin in the brain lysate of WT, Picalm+/−, Tg30 and Tg30xPicalm+/−. **b**, **c** Quantification of Beclin1 and LC3-II normalised to actin is shown. 100% is given to the average of WT. There was a significant decrease of Beclin1 in Tg30xPicalm+/− compared to WT mice and a significant increase of LC3-II in Tg30xPicalm+/− compared to WT and Picalm+/− mice. **d**–**g** Representative pictures of the pons of WT (**d**), Picalm+/− (**e**), Tg30 (**f**) and Tg30xPicalm+/− (**g**) immunostained for p62. 10-month-old male mice were analysed (WT, $n=2$, Picalm+/−, $n=2$, Tg30 $n=12$ and Tg30xPicalm+/−, $n=9$). Scale bar 10 µm. **h** Quantitative analysis of the number of p62 positive structures showed a significant increase in the pons of Tg30 and Tg30xPicalm+/−. In Tg30xPicalm+/−, there were more numerous p62 positive structures than in Tg30. Data are represented as mean +/− SEM (*$p<0.05$, **$p<0.01$, ***$p<0.001$)

GSK3ß and had augmented cdk5 activity due to conversion from p35 to p25.

Discussion

Aggravated motor phenotype and tau pathology in Tg30xPicalm+/− mice

In this work, we report that soluble PICALM protein was decreased and autophagy was deregulated in human FTLD-tau-*MAPT* brains. To analyse the effect of PICALM reduction on tau pathology progression, we created a novel tau mouse line Tg30×Picalm+/−. Picalm haploinsufficiency aggravated brain atrophy, motor deficits and tau pathology in Tg30×Picalm+/− mice compared to Tg30 littermates. Tau hyperphosphorylation was exacerbated as detected by anti-phosphotau AT8 or pSer422 antibodies in Tg30×Picalm+/− mouse brains compared to Tg30. The levels of sarkosyl-insoluble tau proteins and Gallyas-positive NFTs were increased in the cortex and pons of Tg30×Picalm+/− mice compared to Tg30 littermates. The increased tau pathology

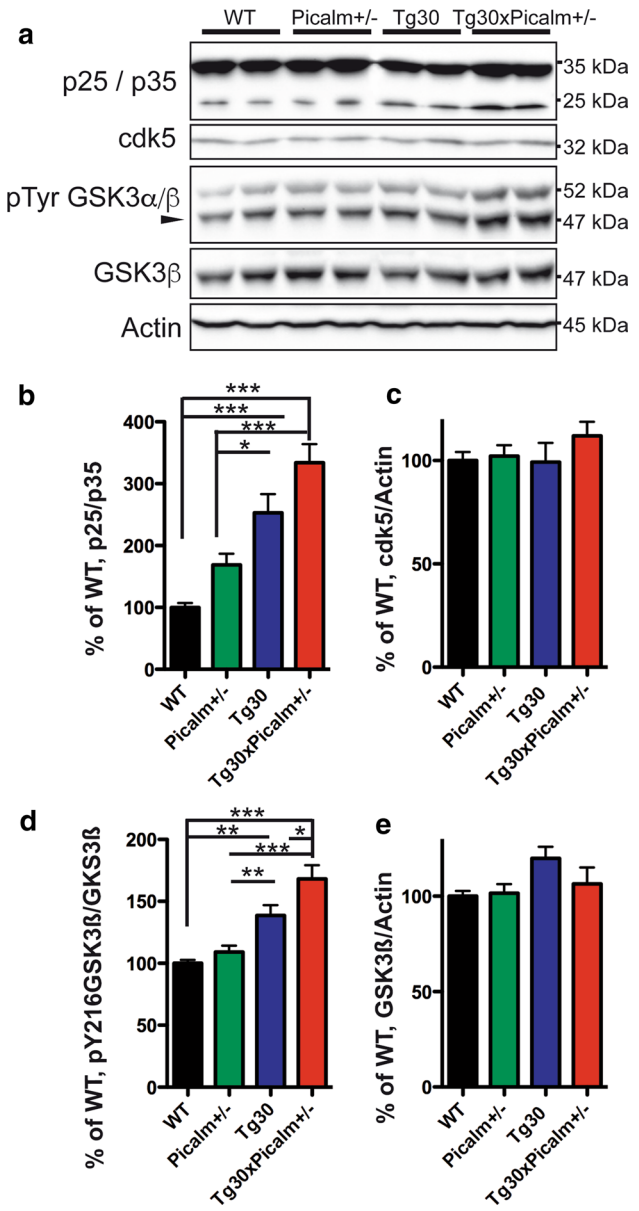

Fig. 7 The level of p25 and activated GSK3ß is increased in Tg30xPicalm+/− compared to Tg30. **a** Sex-matched 10-month-old mouse brains were analysed by WB ($n=12$ per genotype). WB analysis showing the expression of p25/p35, cdk5, pTyr216 GSK3ß, total GSK3ß and actin in the brain lysate of WT, Picalm+/−, Tg30 and Tg30xPicalm+/−. Arrowhead shows pTyr216 GSK3ß. **b** The ratio of p25 normalised to p35 was increased in Tg30xPicalm+/− mice. **c** The level of cdk5 was not significantly different. **d** The active form of GSK3ß phosphorylated at Tyr216 detected at 47 kDa was increased in Tg30xPicalm+/− mice compared to the other genotypes. **e** There was no increase in the total protein level of GSK3ß. $*p<0.05$, $**p<0.01$ and $***p<0.001$ by one-way ANOVA with Turkey post-tests

in the motor cortex and brainstem is expected to contribute to the accelerated motor phenotype observed in Tg30xPicalm+/− mice. Tg30 develops tau pathology in an age-dependent manner and the phenotypic differences between Tg30 and Tg30×Picalm+/− became significant only around 9 months, a relatively late adult stage. This indicates that Picalm reduction had an age-related effect correlated with development of tau pathology.

Reduction of PICALM in the human FTLD-tau-*MAPT* brain and in the Tg30 tauopathy model

We observed that PICALM protein was significantly reduced in the affected brain areas of FTLD-tau-*MAPT* patients down to 42.5%. Such reduction was consistently observed in the 5 FTLD-tau-*MAPT* cases in spite of their heterogeneous neuropathological features, variations of phosphorylated tau levels and distinct interactions between PICALM and tau. Such reduction of soluble PICALM protein level and alteration in protein solubility was also observed in sporadic tauopathies without Aß pathology as CBD and PiD [6]. We also observed a significant reduction of Picalm protein in the RIPA-soluble fraction of the Tg30 mouse brain down to 86%. Distinct mechanisms might explain this reduction. First, PICALM is a substrate of calpain and caspase-3 [3, 28, 46] that are activated in AD and in primary tauopathies [1, 21, 47, 54, 60]. PICALM protein reduction may thus be secondary to an increased proteolysis in these tauopathies. We confirmed that a Picalm-positive species around 50 kDa was more abundant in the brain lysates of Tg30 than in those of WT mice, supporting the hypothesis of an increased Picalm proteolysis in Tg30 mouse brains. Second, one proportion of Picalm may be sequestered in large tau aggregates via direct interaction between tau and Picalm as observed by double immunofluorescence staining in AD [3], in other sporadic tauopathies such as PiD, PSP [6], FTLD-tau-*MAPT*-L266V and in Tg30 mouse brains. Third, under pathological conditions, Picalm protein may undergo post-translational modifications. Some post-translational modifications such as oxidation and lipidation alter protein solubility [22, 52]. Picalm protein reduction in Tg30 was somehow much less remarkable than in human FTLD-tau-*MAPT* cases. This may be related to the fact that neurons may undergo injuries for a longer period in human FTLD-tau-*MAPT* than in transgenic tau mice.

It has to be noted that the rs3851179^{A}, highly validated *PICALM* protective variant for LOAD susceptibility, is associated with higher PICALM expression than non-protective rs3851179^{G} in endothelial cells derived from induced pluripotent stem cells (iPSC) [65]. Nonetheless, no association has been found between SNPs of *PICALM* and susceptibility to FTLD-tau in GWAS and epigenome-wide association studies (EWAS) up to today [10, 56]. Our results in FTLD-tau-*MAPT* and Tg30xPicalm+/− mice nevertheless suggest that Picalm reduction, either primary or secondary, might have an amplification effect on tau pathology progression, e.g. by further autophagy impairment.

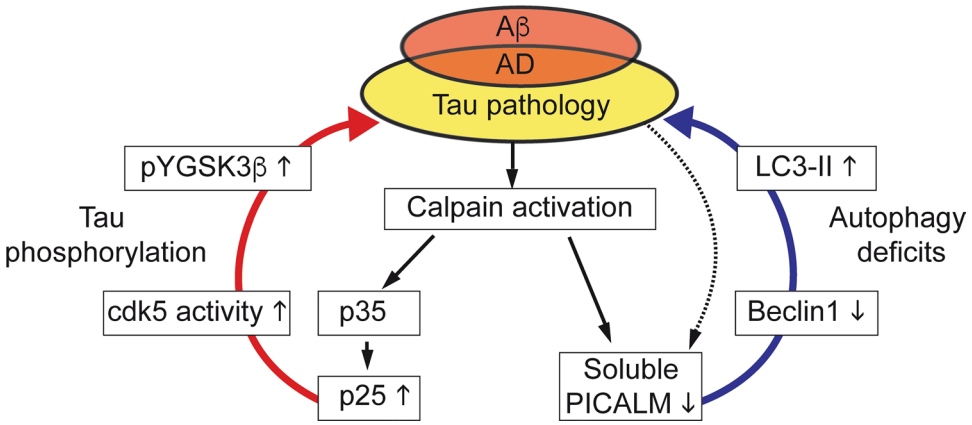

Fig. 8 Schematic summary of our hypothesis linking PICALM reduction and tau pathology. Soluble PICALM is reduced in the tauopathy brain including familial FTLD-tau-*MAPT*, sporadic tauopathies or AD with Aß pathology. In multiple tauopathy brains, calpain is activated and cleaves its substrates including PICALM and p35. Increase of p25 leads to further hyperphosphorylation of tau by cdk5 and GSK3ß (red arrow). Soluble PICALM protein level is further reduced due to cleavage by caspase-3, sequestration by pathological tau and/or other mechanisms as discussed (dotted arrow). Reduction of soluble PICALM further drives autophagy deficits via reduction of Beclin1 and accumulation of LC3-II (blue arrow). Reduction of soluble PICALM is considered to eventually have an amplifying role in a feedback loop increasing pathology

Autophagy deficits in FTLD-tau-*MAPT* and in Tg30xPicalm+/− mice

Loss of autophagy in the central nervous system (CNS) causes neurodegeneration in mice as observed in the conditional *Atg7* (autophagy-related 7)-deficient mice [30]. A clear link between autophagy and tau pathology is confirmed by pharmacological autophagy activation alleviating tau pathology in transgenic tau mice [18, 48]. Interestingly, we confirmed a reduction of autophagy initiation marker Beclin1 and a significant increase of autophagy flux marker LC3-II in the human FTLD-tau-*MAPT* brain [6], supporting the link between autophagy deficit and tau pathology.

Although Picalm+/− mice have slightly reduced survival (not significant when compared to WT), Picalm+/− mice exhibit no clear phenotype on body weight, body gait, motor phenotype, at least up to 10 months. It is not surprising that Picalm+/− mice did not show any alteration in autophagy, because hemizygous loss of most of the autophagy-related genes has generally no or minor effect on autophagy in mice. It is hypothesized that the single wild-type allele, remaining in Picalm+/− mice, is sufficient to maintain its function for autophagy. Contrary to Picalm+/− and Tg30 mice, there was a significant decrease of autophagy initiation marker Beclin1 in Tg30×Picalm+/− compared to WT littermates. We also observed a significant increase of autophagy flux marker LC3-II in Tg30×Picalm+/− mice compared to WT and Picalm+/− mice. Since the autophagy initiation was reduced in Tg30×Picalm+/−, the increase of LC3-II was supposed to reflect a reduction of autophagosome degradation. Our present data on Tg30×Picalm+/− mice are consistent with the previously reported effect of PICALM knock down leading to reduction of autophagy initiation marker Beclin1 and accumulation of autophagy flux marker LC3-II in cultured cells [38]. An excess of autophagosomes in affected neurons are one of the hallmarks of AD. Defects in autophagosome removal may play a role in AD pathophysiology [40]. Decreased autophagy function accelerates both WT and mutant tau accumulation [62]. Autophagy impairment in Tg30×Picalm+/− mice might be responsible for the increased tau pathology in this line, e.g. by impairing clearance of abnormal tau. Accumulation of abnormal tau might also overload more quickly autophagy machinery and exhaust autophagy pathway in Tg30×Picalm+/− mice with a reduced level of Picalm.

Kinase activation is increased in Tg30xPicalm+/− mouse brains

Tau is a substrate of both cdk5 and GSK3ß [23]. Conversion from p35 to p25 is due to proteolysis by calpain [34] and the cleaved p25 fragment was increased in Tg30×Picalm+/− mouse brains. Increased level of the active form of GSK3ß was also observed in Tg30×Picalm+/− mouse brains. Increased activity of both kinases that we observed may drive accelerated phosphorylation of tau in Tg30×Picalm+/− mouse brains. Increased cdk5/p25 activity significantly increases tau pathology progression in wild-type non-mutant tau [14] or in mutant tau mouse brains [41]. p25 overexpression in mouse brains also leads to increased activity of GSK3ß [41, 44]. Since GSK3β phosphorylation of tau is enhanced by prior phosphorylation with cdk5, tau phosphorylation by cdk5 may further increase

the total phosphorylation of tau by facilitating subsequent phosphorylation with GSK3β [7, 36, 50].

Our data implicate that reduced expression of functional Picalm, more pronounced in Tg30×Picalm+/− than in Tg30 mice, is a sensitizing factor responsible for increased tau pathology. In AD and multiple tauopathies, calpain is abnormally activated (Fig. 8) [1, 16, 47]. It is plausible that activation of the calpain cascade in the Tg30 tauopathy model also leads to proteolysis of both Picalm and p35. Conversion of p35 to p25 further increases tau phosphorylation by cdk5 [43], and aberrant Picalm reduction decreases autophagy-mediated tau degradation [38]. Hemizygous Picalm loss in Tg30×Picalm+/− mouse brains may further aggravate this feedback loop caused by calpain-mediated proteolysis of both p35 and Picalm, leading to more pronounced motor phenotype, tau pathology and brain weight loss compared to Tg30.

We acknowledge that there are several limitations in this study. First, Tg30×Picalm+/− model is focusing on the roles of Picalm on tau pathology progression in an FTLD-tau-*MAPT* murine model and does not allow to extend our knowledge of the role of Picalm in Aß production or clearance as implicated in AD. Previously, three independent groups have reported that PICALM modulates amyloid pathology via autophagy cascade, gamma secretase internalisation and Aß transcytosis [27, 58, 65]. PICALM thus seems to have a significant impact on development Aß pathology. Second, Tg30 transgenic mice that we used in this study overexpress a human double mutant tau protein. Such cell autonomous tau pathology caused by transgenic tau may not necessarily reflect usual biological processes of tau pathology progression in the human brain of tauopathies. In AD brains, tau pathology progression follows neuroanatomically connected pathways and potential pathological tau transmission involves tau release and uptake in a Prion-like manner [12]. It is presumed that PICALM may as well play an important role in endocytosis of pathological tau via clathrin-mediated endocytosis [64], where PICALM should play a critical role as clathrin adaptor [57]. However, we believe that this Tg30×Picalm+/− model is important since Picalm reduction observed in human post-mortem FTLD-tau-*MAPT* brains was mimicked in a tauopathy model. This model may thus provide useful information regarding the role of Picalm in tau degradation via autophagy pathway.

Direct association between tau and the proteins coded by the LOAD susceptibility genes

While there is less correlation between amyloid pathology and cognitive loss in AD brains, there is a significant and stronger correlation between tau accumulation and clinical signs [39]. Interestingly, increasing evidence suggests that some of the most significant LOAD susceptibility genes revealed by GWAS [33] code for proteins that are involved in Aß pathology (e.g. APOE [26], PICALM [27, 58, 65] and CLU [63]) as well as in tau pathology via direct interaction with tau (e.g. APOE [53], BIN1 [11], PICALM [3], CLU [66] and PTK2B [15]). Our present study on PICALM supports the hypothesis that one of the common key cascades of LOAD may be the modulation of tau pathology and tau-mediated neurodegeneration, as observed in the experimental models for APOE and BIN1 [13, 51].

Acknowledgements J.P.B was supported by grants from the Belgian Fonds de la Recherche Scientifique Médicale (T.0023.15, T0027.19), the Fund Aline (King Baudoin Foundation). JPB and KL were supported by the Belgian Alzheimer Research Foundation (SAO-FRA) (14001), and the Génicot Fund (ULB). C.D and M.C.P were supported by "Investissements d'avenir" of INSERM (ANR-10-IAIHU-06). CD was supported by France Alzheimer. K.S. is supported by the University of Antwerp Research Fund and SAO-FRA. The brain tissues were provided by the Brainbank NeuroCEB Neuropathology Network (funded by France Parkinson, ARSEP, CSC patients Associations, Fondation Vaincre Alzheimer, ARSLA, DFT France) and the NeuroLHNN biobank (BB190052). We thank Dr Sabrina Turbant for human tissue preparation and the NeuroCEB Neuropathology network: Dr Franck Letournel (CHU Angers), Dr Marie-Laure Martin-Négrier (CHU Bordeaux), Pr Françoise Chapon (CHU Caen), Pr Catherine Godfraind (CHU Clermont-Ferrand), Pr Claude-Alain Maurage (CHU Lille), Dr Vincent Deramecourt (CHU Lille), Dr David Meyronnet (CHU Lyon), Dr Nathalie Streichenberger (CHU Lyon), Dr André Maues de Paula (CHU Marseille), Pr Valérie Rigau (CHU Montpellier), Dr Fanny Vandenbos-Burel (Nice), Pr Charles Duyckaerts (CHU PS Paris), Pr Danielle Seilhean (CHU PS, Paris), Dr Susana Boluda (CHU PS, Paris), Dr Isabelle Plu (CHU PS, Paris), Dr Serge Milin (CHU Poitiers), Dr Dan Christian Chiforeanu (CHU Rennes), Pr Annie Laquerrière (CHU Rouen), Dr Béatrice Lannes (CHU Strasbourg). We also thank Dr Peter Davis (The Feinstein Institute for Medical Research, New York) for PHF1 antibody and Drs Masato Hasegawa and Michel Goedert (Cambridge, UK) for AP422 antibody.

References

1. Adamec E, Mohan P, Vonsattel JP, Nixon RA (2002) Calpain activation in neurodegenerative diseases: confocal immunofluorescence study with antibodies specifically recognizing the active form of calpain 2. Acta Neuropathol 104:92–104
2. Ahmed Z, Bigio EH, Budka H, Dickson DW, Ferrer I, Ghetti B et al (2013) Globular glial tauopathies (GGT): consensus recommendations. Acta Neuropathol 126:537–544
3. Ando K, Brion JP, Stygelbout V, Suain V, Authelet M, Dedecker R et al (2013) Clathrin adaptor CALM/PICALM is associated with neurofibrillary tangles and is cleaved in Alzheimer's brains. Acta Neuropathol 125:861–878
4. Ando K, Kabova A, Stygelbout V, Leroy K, Heraud C, Frederick C et al (2014) Vaccination with sarkosyl insoluble PHF-Tau decrease neurofibrillary tangles formation in aged tau transgenic mouse model: a pilot study. J Alzheimers Dis 40:S135–S145
5. Ando K, Leroy K, Heraud C, Yilmaz Z, Authelet M, Suain V et al (2011) Accelerated human mutant tau aggregation by knocking out murine tau in a transgenic mouse model. Am J Pathol 178:803–816
6. Ando K, Tomimura K, Sazdovitch V, Suain V, Yilmaz Z, Authelet M et al (2016) Level of PICALM, a key component of

clathrin-mediated endocytosis, is correlated with levels of phosphotau and autophagy-related proteins and is associated with tau inclusions in AD, PSP and Pick disease. Neurobiol Dis 94:32–43
7. Arioka M, Tsukamoto M, Ishiguro K, Kato R, Sato K, Imahori K et al (1993) Tau protein kinase II is involved in the regulation of the normal phosphorylation state of tau protein. J Neurochem 60:461–468
8. Brion JP, Hanger DP, Bruce MT, Couck AM, Flament-Durand J, Anderton BH (1991) Tau in Alzheimer neurofibrillary tangles. N- and C-terminal regions are differentially associated with paired helical filaments and the location of a putative abnormal phosphorylation site. Biochem J 273:127–133
9. Brion JP, Hanger DP, Couck AM, Anderton BH (1991) A68 proteins in Alzheimer's disease are composed of several tau isoforms in a phosphorylated state which affects their electrophoretic mobilities. Biochem J 279(Pt 3):831–836
10. Broce I, Karch CM, Wen N, Fan CC, Wang Y, Tan CH et al (2018) Immune-related genetic enrichment in frontotemporal dementia: An analysis of genome-wide association studies. PLoS Med 15:e1002487
11. Chapuis J, Hansmannel F, Gistelinck M, Mounier A, Van Cauwenberghe C, Kolen KV et al (2013) Increased expression of BIN1 mediates Alzheimer genetic risk by modulating tau pathology. Mol Psychiatry 18:1225–1234
12. Clavaguera F, Bolmont T, Crowther RA, Abramowski D, Frank S, Probst A et al (2009) Transmission and spreading of tauopathy in transgenic mouse brain. Nat Cell Biol 11:909–913
13. Crotti A, Sait HR, McAvoy KM, Estrada K, Ergun A, Szak S et al (2019) BIN1 favors the spreading of Tau via extracellular vesicles. Sci Rep 9:9477
14. Cruz JC, Tseng HC, Goldman JA, Shih H, Tsai LH (2003) Aberrant Cdk5 activation by p25 triggers pathological events leading to neurodegeneration and neurofibrillary tangles. Neuron 40:471–483
15. Dourlen P, Fernandez-Gomez FJ, Dupont C, Grenier-Boley B, Bellenguez C, Obriot H et al (2017) Functional screening of Alzheimer risk loci identifies PTK2B as an in vivo modulator and early marker of Tau pathology. Mol Psychiatry 22:874–883
16. Ferreira A, Bigio EH (2011) Calpain-mediated tau cleavage: a mechanism leading to neurodegeneration shared by multiple tauopathies. Mol Med 17:676–685
17. Forrest SL, Kril JJ, Stevens CH, Kwok JB, Hallupp M, Kim WS et al (2018) Retiring the term FTDP-17 as MAPT mutations are genetic forms of sporadic frontotemporal tauopathies. Brain 141:521–534
18. Frederick C, Ando K, Leroy K, Heraud C, Suain V, Buee L et al (2015) Rapamycin ester analog CCI-779/Temsirolimus alleviates tau pathology and improves motor deficit in mutant tau transgenic mice. J Alzheimers Dis 44:1145–1156
19. Goedert M, Jakes R, Vanmechelen E (1995) Monoclonal antibody AT8 recognises tau protein phosphorylated at both serine 202 and threonine 205. Neurosci Lett 189:167–169
20. Greenberg SG, Davies P (1990) A preparation of Alzheimer paired helical filaments that displays distinct tau proteins by polyacrylamide gel electrophoresis. Proc Natl Acad Sci USA 87:5827–5831
21. Grynspan F, Griffin WR, Cataldo A, Katayama S, Nixon RA (1997) Active site-directed antibodies identify calpain II as an early-appearing and pervasive component of neurofibrillary pathology in Alzheimer's disease. Brain Res 763:145–158
22. Hang HC, Linder ME (2011) Exploring protein lipidation with chemical biology. Chem Rev 111:6341–6358
23. Hanger DP, Anderton BH, Noble W (2009) Tau phosphorylation: the therapeutic challenge for neurodegenerative disease. Trends Mol Med 15:112–119
24. Harold D, Abraham R, Hollingworth P, Sims R, Gerrish A, Hamshere ML et al (2009) Genome-wide association study identifies variants at CLU and PICALM associated with Alzheimer's disease. Nat Genet 41:1088–1093
25. Hasegawa M, Jakes R, Crowther RA, Lee VM, Ihara Y, Goedert M (1996) Characterization of mAb AP422, a novel phosphorylation-dependent monoclonal antibody against tau protein. FEBS Lett 384:25–30
26. Huang YA, Zhou B, Wernig M, Sudhof TC (2017) ApoE2, ApoE3, and ApoE4 differentially stimulate APP transcription and abeta secretion. Cell 168(427–441):e421
27. Kanatsu K, Morohashi Y, Suzuki M, Kuroda H, Watanabe T, Tomita T et al (2014) Decreased CALM expression reduces Abeta42 to total Abeta ratio through clathrin-mediated endocytosis of gamma-secretase. Nat Commun 5:3386
28. Kim JA, Kim HL (2001) Cleavage of purified neuronal clathrin assembly protein (CALM) by caspase 3 and calpain. Exp Mol Med 33:245–250
29. Kobayashi T, Ota S, Tanaka K, Ito Y, Hasegawa M, Umeda Y et al (2003) A novel L266V mutation of the tau gene causes frontotemporal dementia with a unique tau pathology. Ann Neurol 53:133–137
30. Komatsu M, Waguri S, Chiba T, Murata S, Iwata J, Tanida I et al (2006) Loss of autophagy in the central nervous system causes neurodegeneration in mice. Nature 441:880–884
31. Kuninaka N, Kawaguchi M, Ogawa M, Sato A, Arima K, Murayama S et al (2015) Simplification of the modified Gallyas method. Neuropathology 35:10–15
32. Lambert JC, Heath S, Even G, Campion D, Sleegers K, Hiltunen M et al (2009) Genome-wide association study identifies variants at CLU and CR1 associated with Alzheimer's disease. Nat Genet 41:1094–1099
33. Lambert JC, Ibrahim-Verbaas CA, Harold D, Naj AC, Sims R, Bellenguez C et al (2013) Meta-analysis of 74,046 individuals identifies 11 new susceptibility loci for Alzheimer's disease. Nat Genet 45:1452–1458
34. Lee MS, Kwon YT, Li M, Peng J, Friedlander RM, Tsai LH (2000) Neurotoxicity induces cleavage of p35 to p25 by calpain. Nature 405:360–364
35. Leroy K, Bretteville A, Schindowski K, Gilissen E, Authelet M, De Decker R et al (2007) Early axonopathy preceding neurofibrillary tangles in mutant tau transgenic mice. Am J Pathol 171:976–992
36. Li T, Hawkes C, Qureshi HY, Kar S, Paudel HK (2006) Cyclin-dependent protein kinase 5 primes microtubule-associated protein tau site-specifically for glycogen synthase kinase 3beta. Biochemistry 45:3134–3145
37. Miller SE, Mathiasen S, Bright NA, Pierre F, Kelly BT, Kladt N et al (2015) CALM regulates clathrin-coated vesicle size and maturation by directly sensing and driving membrane curvature. Dev Cell 33:163–175
38. Moreau K, Fleming A, Imarisio S, Lopez Ramirez A, Mercer JL, Jimenez-Sanchez M et al (2014) PICALM modulates autophagy activity and tau accumulation. Nat Commun 5:4998
39. Nelson PT, Alafuzoff I, Bigio EH, Bouras C, Braak H, Cairns NJ et al (2012) Correlation of Alzheimer disease neuropathologic changes with cognitive status: a review of the literature. J Neuropathol Exp Neurol 71:362–381
40. Nixon RA (2013) The role of autophagy in neurodegenerative disease. Nat Med 19:983–997
41. Noble W, Olm V, Takata K, Casey E, Mary O, Meyerson J et al (2003) Cdk5 is a key factor in tau aggregation and tangle formation in vivo. Neuron 38:555–565
42. Otvos L Jr, Feiner L, Lang E, Szendrei GI, Goedert M, Lee VM (1994) Monoclonal antibody PHF-1 recognizes tau protein phosphorylated at serine residues 396 and 404. J Neurosci Res 39:669–673

43. Patrick GN, Zukerberg L, Nikolic M, de la Monte S, Dikkes P, Tsai LH (1999) Conversion of p35 to p25 deregulates Cdk5 activity and promotes neurodegeneration. Nature 402:615–622
44. Plattner F, Angelo M, Giese KP (2006) The roles of cyclin-dependent kinase 5 and glycogen synthase kinase 3 in tau hyperphosphorylation. J Biol Chem 281:25457–25465
45. Popovic M, Fabjan A, Mraz J, Magdic J, Glavac D, Zupan A et al (2014) Tau protein mutation P364S in two sisters: clinical course and neuropathology with emphasis on new, composite neuronal tau inclusions. Acta Neuropathol 128:155–157
46. Rudinskiy N, Grishchuk Y, Vaslin A, Puyal J, Delacourte A, Hirling H et al (2009) Calpain hydrolysis of alpha- and beta2-adaptins decreases clathrin-dependent endocytosis and may promote neurodegeneration. J Biol Chem 284:12447–12458
47. Saito K, Elce JS, Hamos JE, Nixon RA (1993) Widespread activation of calcium-activated neutral proteinase (calpain) in the brain in Alzheimer disease: a potential molecular basis for neuronal degeneration. Proc Natl Acad Sci USA 90:2628–2632
48. Schaeffer V, Lavenir I, Ozcelik S, Tolnay M, Winkler DT, Goedert M (2012) Stimulation of autophagy reduces neurodegeneration in a mouse model of human tauopathy. Brain 135:2169–2177
49. Schindowski K, Bretteville A, Leroy K, Begard S, Brion JP, Hamdane M et al (2006) Alzheimer's disease-like tau neuropathology leads to memory deficits and loss of functional synapses in a novel mutated tau transgenic mouse without any motor deficits. Am J Pathol 169:599–616
50. Sengupta A, Wu Q, Grundke-Iqbal I, Iqbal K, Singh TJ (1997) Potentiation of GSK-3-catalyzed Alzheimer-like phosphorylation of human tau by cdk5. Mol Cell Biochem 167:99–105
51. Shi Y, Yamada K, Liddelow SA, Smith ST, Zhao L, Luo W et al (2017) ApoE4 markedly exacerbates tau-mediated neurodegeneration in a mouse model of tauopathy. Nature 549:523–527
52. Snyder SW, Ladror US, Wade WS, Wang GT, Barrett LW, Matayoshi ED et al (1994) Amyloid-beta aggregation: selective inhibition of aggregation in mixtures of amyloid with different chain lengths. Biophys J 67:1216–1228
53. Strittmatter WJ, Saunders AM, Goedert M, Weisgraber KH, Dong LM, Jakes R et al (1994) Isoform-specific interactions of apolipoprotein E with microtubule-associated protein tau: implications for Alzheimer disease. Proc Natl Acad Sci USA 91:11183–11186
54. Su JH, Zhao M, Anderson AJ, Srinivasan A, Cotman CW (2001) Activated caspase-3 expression in Alzheimer's and aged control brain: correlation with Alzheimer pathology. Brain Res 898:350–357
55. Suzuki M, Tanaka H, Tanimura A, Tanabe K, Oe N, Rai S et al (2012) The clathrin assembly protein PICALM is required for erythroid maturation and transferrin internalization in mice. PLoS ONE 7:e31854
56. Taskesen E, Mishra A, van der Sluis S, Ferrari R, International FTDGC, Veldink JH et al (2017) Susceptible genes and disease mechanisms identified in frontotemporal dementia and frontotemporal dementia with Amyotrophic Lateral Sclerosis by DNA-methylation and GWAS. Sci Rep 7:8899
57. Tebar F, Bohlander SK, Sorkin A (1999) Clathrin assembly lymphoid myeloid leukemia (CALM) protein: localization in endocytic-coated pits, interactions with clathrin, and the impact of overexpression on clathrin-mediated traffic. Mol Biol Cell 10:2687–2702
58. Tian Y, Chang JC, Fan EY, Flajolet M, Greengard P (2013) Adaptor complex AP2/PICALM, through interaction with LC3, targets Alzheimer's APP-CTF for terminal degradation via autophagy. Proc Natl Acad Sci USA 110:17071–17076
59. Tian Y, Chang JC, Greengard P, Flajolet M (2014) The convergence of endosomal and autophagosomal pathways: implications for APP-CTF degradation. Autophagy 10:694–696
60. Tsuji T, Shimohama S, Kimura J, Shimizu K (1998) m-Calpain (calcium-activated neutral proteinase) in Alzheimer's disease brains. Neurosci Lett 248:109–112
61. Vergara C, Houben S, Suain V, Yilmaz Z, De Decker R, Vanden Dries V et al (2019) Amyloid-beta pathology enhances pathological fibrillary tau seeding induced by Alzheimer PHF in vivo. Acta Neuropathol 137:397–412
62. Wang Y, Martinez-Vicente M, Kruger U, Kaushik S, Wong E, Mandelkow EM et al (2009) Tau fragmentation, aggregation and clearance: the dual role of lysosomal processing. Hum Mol Genet 18:4153–4170
63. Wojtas AM, Kang SS, Olley BM, Gatherer M, Shinohara M, Lozano PA et al (2017) Loss of clusterin shifts amyloid deposition to the cerebrovasculature via disruption of perivascular drainage pathways. Proc Natl Acad Sci USA 114:E6962–E6971
64. Wu JW, Herman M, Liu L, Simoes S, Acker CM, Figueroa H et al (2013) Small misfolded Tau species are internalized via bulk endocytosis and anterogradely and retrogradely transported in neurons. J Biol Chem 288:1856–1870
65. Zhao Z, Sagare AP, Ma Q, Halliday MR, Kong P, Kisler K et al (2015) Central role for PICALM in amyloid-beta blood-brain barrier transcytosis and clearance. Nat Neurosci 18:978–987
66. Zhou Y, Hayashi I, Wong J, Tugusheva K, Renger JJ, Zerbinatti C (2014) Intracellular clusterin interacts with brain isoforms of the bridging integrator 1 and with the microtubule-associated protein Tau in Alzheimer's disease. PLoS ONE 9:e103187